EPJ Web of Conferences **80**, 00032 (2014)
DOI: 10.1051/epjconf/20148000032

Production of light-flavour hadrons in pp, p–Pb and Pb–Pb collisions at LHC energies measured with ALICE

Francesco Barile[1,a] for the ALICE Collaboration

[1] *Dipartimento Interateneo di Fisica "M. Merlin" and INFN Sezione di Bari, via E. Orabona 4, 70126 Bari, Italy*

Abstract. In the first three years of LHC operation, ALICE has measured identified light-flavour hadrons in a wide transverse momentum range. The measurements have been performed for the three collision systems: pp at $\sqrt{s}$ = 0.9, 2.76 and 7 TeV, p–Pb at $\sqrt{s_{\rm NN}}$ = 5.02 TeV and Pb–Pb at $\sqrt{s_{\rm NN}}$ = 2.76 TeV. The latest results on transverse momentum distributions, particle ratios and integrated production yields are reported.

1 Introduction

Strongly-interacting matter under extreme conditions of high temperature and density can be investigated in ultrarelativistic heavy-ion collisions. The measurement of transverse momentum ($p_{\rm T}$) distributions and yields of identified particles plays a central role in understanding collective and thermal properties of the matter produced in such collisions.
ALICE (A Large Ion Collider Experiment) [1–3] is a general-purpose detector for heavy-ion studies at the CERN LHC (Large Hadron Collider). It has unique particle identification (PID) capabilities among the LHC experiments, allowing for measurements of particles in a wide range in $p_{\rm T}$. The ALICE experiment consists of a central-barrel detector and several forward detector systems. The central barrel, located inside a solenoidal magnet (B = 0.5 T), covers the mid-rapidity region $|\eta| < 0.9$ over the full azimuthal angle. It includes a six-layer high-resolution Inner Tracking System (ITS), a large-volume Time Projection Chamber (TPC), electron and charged-hadron identification detectors which exploit Transition Radiation (TRD) and Time Of Flight (TOF) techniques, respectively. Small-area detectors for high $p_{\rm T}$ particle-identification (HMPID), photon and neutral-meson measurement (PHOS), photon and electron ID and jet reconstruction (EMCal) complement the central barrel. The forward-rapidity system includes a single-arm muon spectrometer covering the pseudorapidity range $-4.0 \leq \eta \leq -2.5$ and several smaller detectors for triggering, multiplicity measurements and centrality determination.

2 Particle identification in ALICE

In this section the particle-identification detectors relevant to the analysis presented here are briefly described. A detailed review of the ALICE experiment and of its PID capabilities can be found in [1–3].

[a] e-mail: francesco.barile@cern.ch

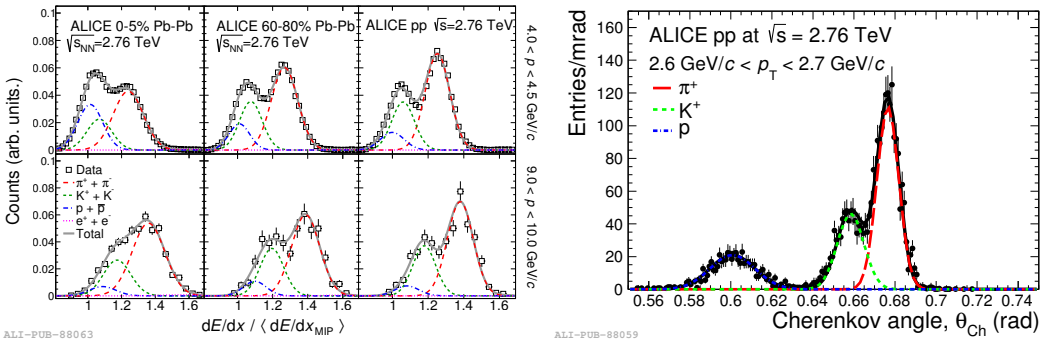

Figure 1. Left: examples of the TPC dE/dx distributions for pp and Pb–Pb (central and peripheral) collisions for two momentum intervals. Right: an example of the Cherenkov angle distribution measured in the HMPID for positive tracks in a narrow p_{T} interval in pp collisions [8].

The ITS is a six-layer silicon detector with radii between 3.9 cm and 43 cm. Four out of the six layers also measure the specific energy loss per unit length (dE/dx) of the particles and are used for particle identification in the non-relativistic region. The TPC is the main central-barrel tracking detector of ALICE. It is a large-volume high-granularity cylindrical detector that provides three-dimensional hit information and dE/dx measurement with up to 159 samples. It can measure charged particle abundances on a statistical basis also in the relativistic rise for momenta up to 50 GeV/c (Figure 1, left). The TOF detector is a large area array devoted to particle identification in the intermediate momentum range up to 2.5 GeV/c for pions and kaons, up to 4 GeV/c for protons. TOF measures the time of flight of the particles coming from the interaction point with a very good resolution (about 120 ps in pp and 85 ps in Pb–Pb collisions). The High Momentum Particle Identification Detector (HMPID) [4] is a single-arm proximity-focusing Ring Imaging Cherenkov detector and consists of seven identical counters covering in total 5% acceptance of the central barrel phase space. It enhances the particle identification capabilities of ALICE at higher momenta: pion and kaons are identified up to 3 GeV/c and protons up to 6 GeV/c (Figure 1, right). The $\mathrm{K}^0_{\mathrm{S}}$ and Λ are identified exploiting their V^0 weak decay topology in the channels $\mathrm{K}^0_{\mathrm{S}} \rightarrow \pi^+\pi^-$ and $\Lambda(\bar{\Lambda}) \rightarrow \mathrm{p}\pi^-(\bar{\mathrm{p}}\pi^+)$. More details on the V^0 reconstruction can be found in [5, 6].

3 Light-flavour hadron production

ALICE has measured the production yields of charged pions, kaons and protons in a wide momentum range and in several colliding systems. The measurements have been performed in pp collisions at different centre-of-mass energies ($\sqrt{s}$ = 0.9 [7], 2.76 [8] and 7 TeV), in p–Pb collisions at $\sqrt{s_{\mathrm{NN}}}$ = 5.02 TeV as a function of charged-particle multiplicity[9] and in Pb–Pb collisions at $\sqrt{s_{\mathrm{NN}}}$ = 2.76 TeV as a function of collision centrality [5].

Figure 2 shows the invariant yields measured in Pb–Pb collisions (0-5% and 60-80% centrality classes) compared to those in pp collisions scaled by the number of binary collisions ($\mathrm{N_{coll}}$) [10, 11]. For peripheral Pb–Pb collisions the shapes of the invariant yields are similar to what is expected for an incoherent superposition of nucleon-nucleon collisions. For central Pb–Pb collisions, the spectra exhibit a reduction in the production of high p_{T} particles with respect to the reference. This feature is interpreted as an effect of parton energy loss in the strongly-interacting medium. For more details on

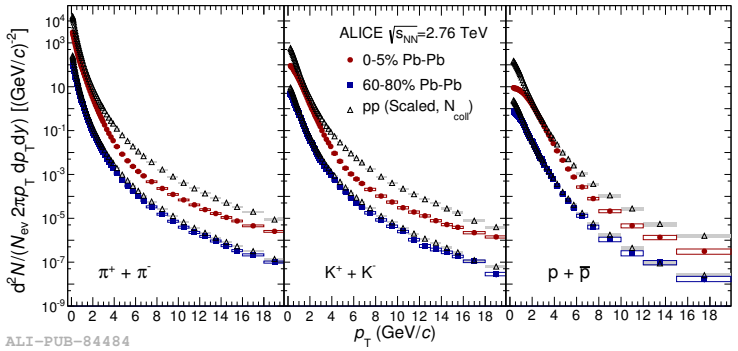

Figure 2. Solid markers show the invariant yields of identified particles in central and peripheral Pb–Pb collisions. Open triangles show the pp reference yields scaled by the average number of nucleon-nucleon collisions for 0-5% (upper) and 60-80% (lower). The statistical and systematic uncertainties are shown as vertical error bars and boxes, respectively [8].

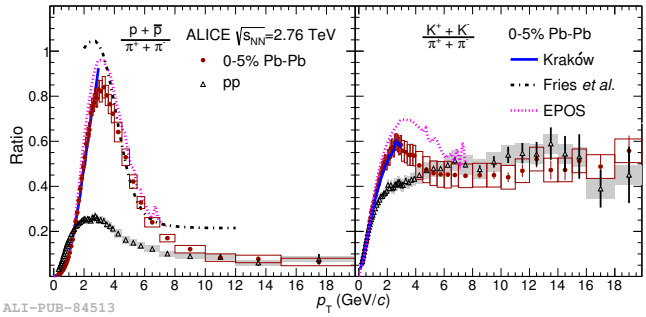

Figure 3. Particle ratios as a function of p_T measured in pp and for most central 0-5% Pb–Pb collisions. Statistical and systematic uncertainties are displayed as vertical error bars and boxes, respectively. The theoretical predictions refer to Pb–Pb collisions [8].

Pb–Pb results see also [12].

Figure 3 shows the proton-to-pion $(p+\bar{p})/(\pi^+ + \pi^-)$ and kaon-to-pion $(K^+ + K^-)/(\pi^+ + \pi^-)$ ratios as a function of p_T. For central Pb–Pb collisions, p/π reaches ~ 0.83 at the maximum around 3 GeV/c and then decreases with increasing p_T. These values are approximately 20% above the peak values measured by PHENIX [13] and STAR [14] in Au–Au collisions at $\sqrt{s_{NN}} = 200$ GeV. In central Pb–Pb collisions, the K/π ratio exhibits a bump at $p_T \sim 3$ GeV/c. This feature is qualitatively described in the models that include coalescence as a mechanism for parton hadronization in the low p_T region. The Kraków [15] hydrodynamic model reproduces the rise of both ratios quantitatively well, while a similar model, HKM [16] that is not shown, does slightly worse. The EPOS [17] event generator that takes into account the interaction between jets and the hydrodynamically expanding medium (radial flow) and does not include coalescence, provides a good qualitative description of the data but tends to overestimate the peaks. For $p_T < 3$ GeV/c, the shape of the proton-to-pion ratio reported here is consistent with the ϕ-meson-to-pion ratio [18]: these results, together with the reasonable description

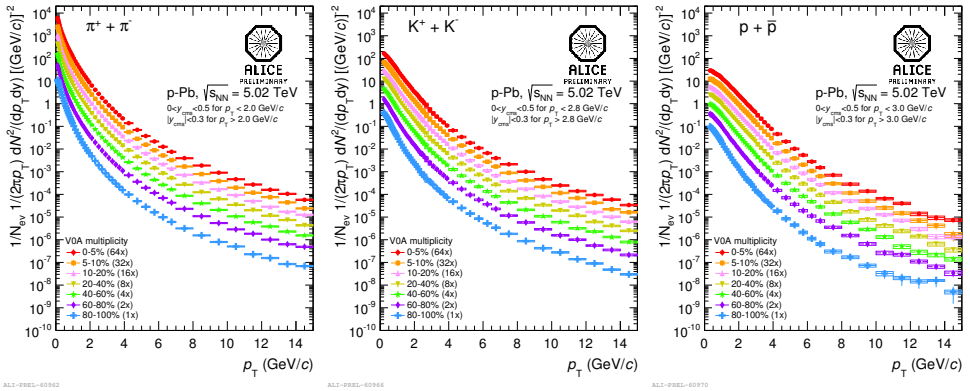

Figure 4. Invariant p_{T}-differential yields of $\pi^{\pm}$, $\mathrm{K}^{\pm}$, $\mathrm{p}(\bar{\mathrm{p}})$ in different V0A multiplicity classes (sum of particle and antiparticle) measured in the rapidity interval $0 < y_{\mathrm{CMS}} < 0.5$. Data are scaled by 2^n factors for better visibility. Statistical (bars) and full systematic (boxes) uncertainties are shown.

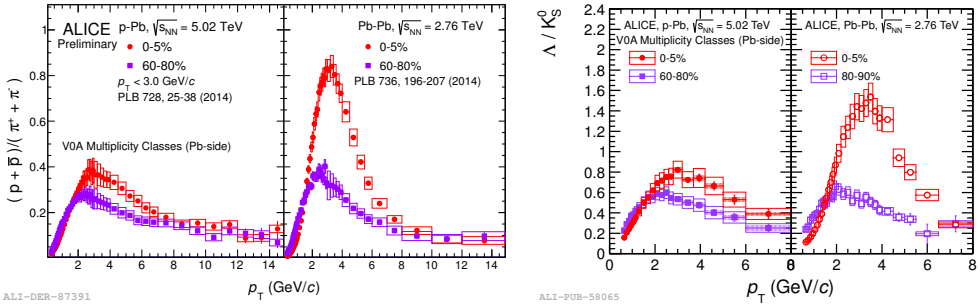

Figure 5. Proton-to-pion and $\Lambda/\mathrm{K}^0_{\mathrm{S}}$ ratios as a function of p_{T} measured in p–Pb and Pb–Pb collisions at $\sqrt{s_{\mathrm{NN}}} = 5.02$ and 2.76 TeV. The systematic and statistical uncertainties are shown as boxes and error bars, respectively.

provided by the EPOS model comparison shown in Figure 3, indicate that the bump could be induced mainly by radial flow, for which the effect depends on the mass of the hadron and not on its quark composition. Above 10 GeV/c both particle ratios behave like those in pp collisions, suggesting that fragmentation dominates the hadron production at high p_{T}.

Figure 4 shows the p_{T}-differential invariant yields of π, K and p (sum of particle and antiparticle) in rapidity interval $0 < y_{\mathrm{CMS}} < 0.5$ for p–Pb collisions at $\sqrt{s_{\mathrm{NN}}} = 5.02$ TeV. The yields are measured in several classes in the event activity, estimated from the multiplicity at forward rapidity (V0A scintillator detector). The p_{T} distributions show a clear evolution, becoming harder as the multiplicity increases. They show a decrease of the slope at low p_{T}, similar to the one observed in heavy-ion collisions, the change being most pronounced for heavier particles (protons): see [9] for more details. The stronger multiplicity dependence of the spectral shapes for the heavier particles is evident when looking at the ratios K/π, p/π and $\Lambda/\mathrm{K}^0_{\mathrm{S}}$. Figure 5 shows the p/$\pi$ and $\Lambda/\mathrm{K}^0_{\mathrm{S}}$ ratios as a function of p_{T} for p–Pb and Pb–Pb collisions: the baryon-to-meson ratio in p–Pb increases with event multiplicity,

qualitatively reminiscent of that in Pb–Pb collisions though with a smaller increase compared with that for heavy-ion collisions. This behaviour can be qualitatively interpreted in terms of collective effects also in p–Pb (smaller radial flow compared to Pb–Pb) or with a different mechanism underlying particle production in the two systems.

4 Summary and conclusions

The most recent results of the ALICE experiment on light-flavour hadron production in pp, in p–Pb and in Pb–Pb collisions have been reported. The transverse momentum spectra for pions, kaons and protons have been measured with ALICE in several colliding systems and energies at the LHC showing the excellent PID capabilities of the experiment. In Pb–Pb, we observe that the proton-to-pion and the kaon-to-pion ratios both exhibit a peak and that at low p_{T}, the rise of both ratios can be well described by hydrodynamic calculations. At higher p_{T}, both ratios are compatible with those measured in pp collisions. The results presented can establish constraints on theoretical modeling for fragmentation and energy loss mechanisms. Recent results from p–Pb collisions have been also reported. The transverse momentum distributions show a clear evolution, becoming harder as the multiplicity increases, similar to the pattern observed in heavy-ion collisions.

References

[1] F. Carminati et al. (ALICE Collaboration), Physics Performance Report, Volume I, J. Phys. G: Nucl. Part. Phys. 30 (2004) 1517-1763.
[2] B. Alessandro et al. (ALICE Collaboration), Physics Performance Report, Volume II, J. Phys. G: Nucl. Part. Phys. 32 (2006) 1295-2040.
[3] K. Aamodt et al. (ALICE Collaboration), J. Instrum. 3 (2008) SO8002.
[4] F. Barile for the ALICE Collaboration, Proceedings of the 13th ICATPP Conference, World Scientific Publishing Co. Pte. Ltd. (2012), 445-449.
[5] B. Abelev et al. (ALICE Collaboration), Phys. Rev. Lett. 111 (2013) 222301.
[6] K. Aamodt, et al. (ALICE Collaboration), Eur. Phys. J. C 71 (2011) 1594.
[7] A. Aamodt et al. (ALICE Collaboration), Eur. Phys. J. C 71 (2011) 1655.
[8] B. Abelev et al. (ALICE Collaboration), Phys. Lett. B 736 (2014) 196-206.
[9] B. Abelev et al. (ALICE Collaboration), Phys. Lett. B 728 (2014) 25-38.
[10] B. Abelev et al. (ALICE Collaboration), Phys. Rev. C 88 (2013) 044909.
[11] B. Abelev et al. (ALICE Collaboration), Eur. Phys. J. C 73 (2013) 2456.
[12] B. Abelev et al. (ALICE Collaboration), Phys. Rev. 88 (2013) 044919.
[13] S. S. Adler et al. (PHENIX Collaboration), Phys. Rev. C 69 (2004) 034909.
[14] B. Abelev et al. (STAR Collaboration), Phys. Rev. C 79 (2009) 034909.
[15] P. Bozek, Phys. Rev. C 85 (2012) 034901.
[16] Y. Karpenko and Y. Sinyukov, J. Phys. G 38 (2011) 124059.
[17] K. Werner, I. Karpenko, M. Bleicher, T. Pierog, and S. Porteboeuf-Houssais, Phys. Rev. C 85 (2012) 064907.
[18] B. Abelev et al. (ALICE Collaboration), (2014) arXiv:1404.0495 [nucl-ex].